

Supporting information for An Organic Ionic Plastic Crystal Electrolyte for Rate Capability and Stability of Ambient Temperature Lithium Batteries

Liyu Jin,^{ab} Patrick C. Howlett,^{*bc} Jennifer M. Pringle,^{bc} Judith Janikowski,^{ab} Michel Armand,^e
Douglas R. MacFarlane^{bd} and Maria Forsyth^{bc}

^a Department of Materials Engineering, Monash University, Clayton, Victoria 3800, Australia

^b ARC Centre of Excellence for Electromaterials Science

^c Institute for Frontier Materials, Deakin University, Burwood Campus, Burwood, Victoria 3125, Australia.

E-mail: patrick.howlett@deakin.edu.au

^d School of Chemistry, Monash University, Clayton, Victoria 3800, Australia

^e CIC Energigune Energy Cooperative Research Centre, C/Albert Einstein 48 CP 01510 Minano, Spain

Fig 2 from the paper is enlarged and plotted in three figures as follows:

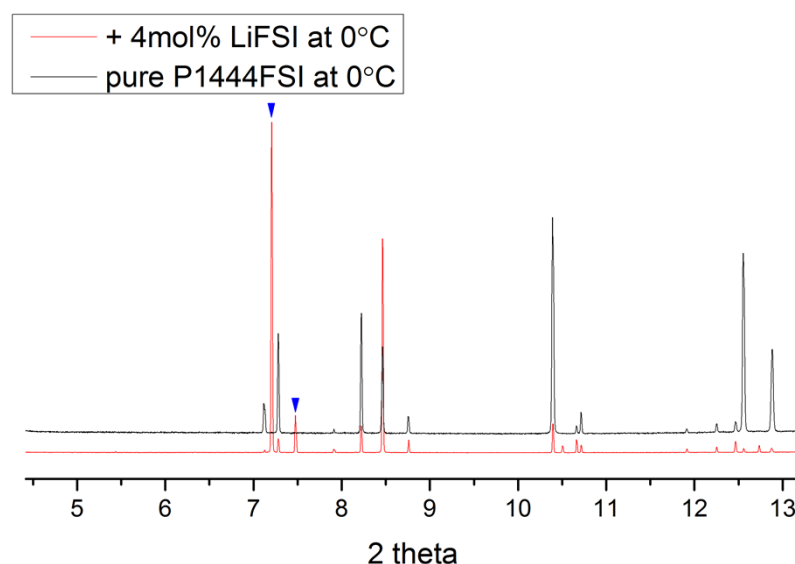


Fig S1 A comparison of XRD patterns with normalized intensities (**2theta from 5 to 13 degree**) for the 4 mol% LiFSI doped sample and the pure sample at **0 °C**. All the peaks from the pure sample can also be found in the doped one, while the two new peaks are marked with blue triangles. Peaks that occur at the same 2theta position but with different normalized intensities may be due to orientational variability of the crystals in the capillaries.

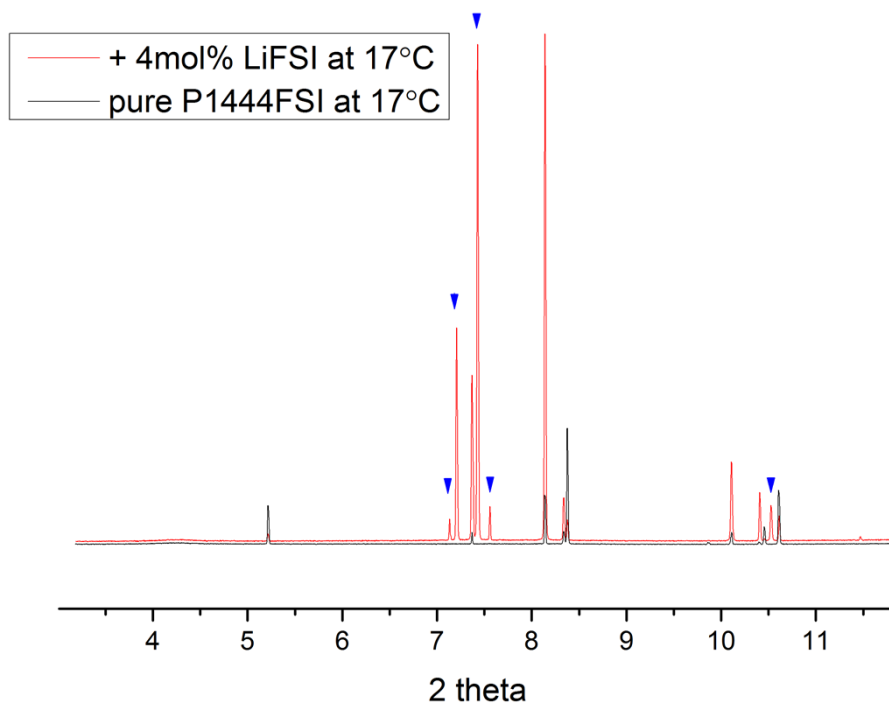


Fig S2 A comparison of XRD patterns with normalized intensities (2theta from 4 to 11 degree) for the 4 mol% LiFSI doped sample and the pure sample at 17 °C. The new peaks are marked with blue triangles.

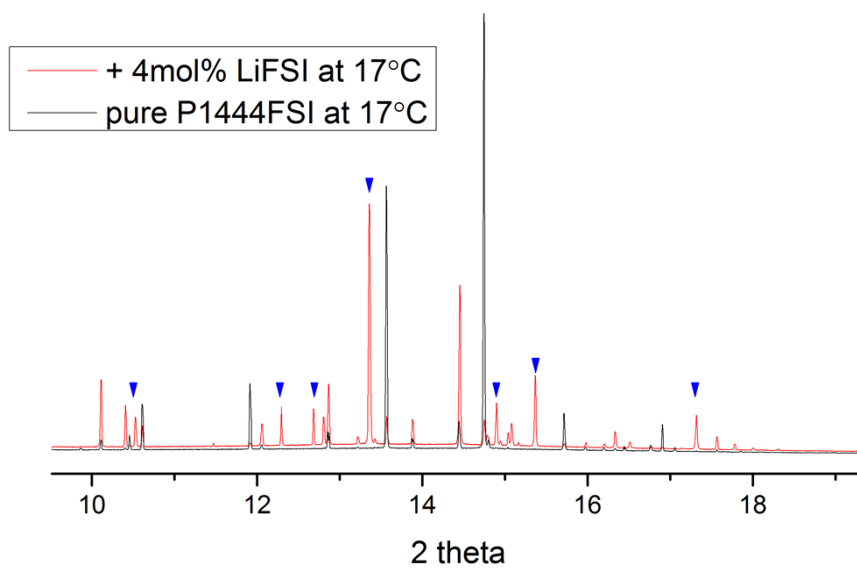


Fig S3 A comparison of XRD patterns with normalized intensities (2theta from 10 to 18 degree) between the 4 mol% LiFSI doped sample and the pure sample at 17 °C. The new peaks are marked with blue triangles.

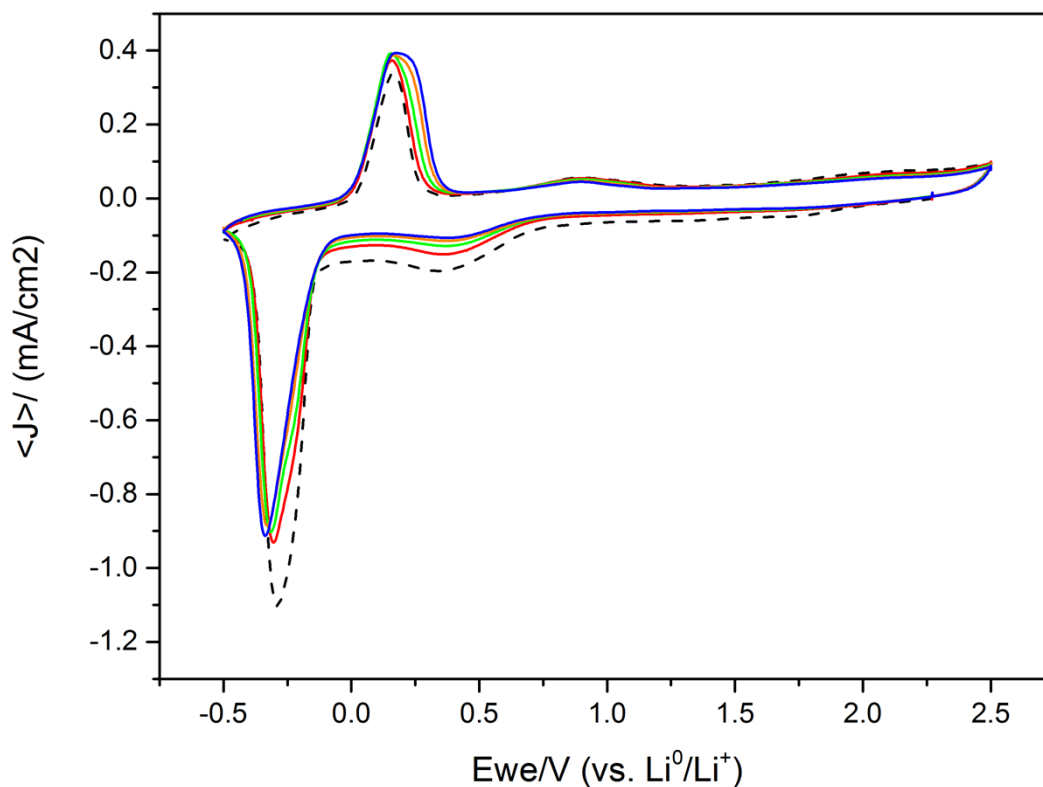


Fig S4 Cyclic voltammograms of 4 mol % LiFSI doped P₁₄₄₄FSI at 20 °C with a scan rate of 50mV s⁻¹. The working electrode was copper and the reference/counter electrode was lithium. This is a repetition of the experiment shown in Fig 4b in the paper but with a low potential cut-off set to -0.5 V from the first cycle.

Nyquist plots (at -10 °C, 20 °C, 30 °C and 40 °C) used for plotting Fig 3 are shown below:

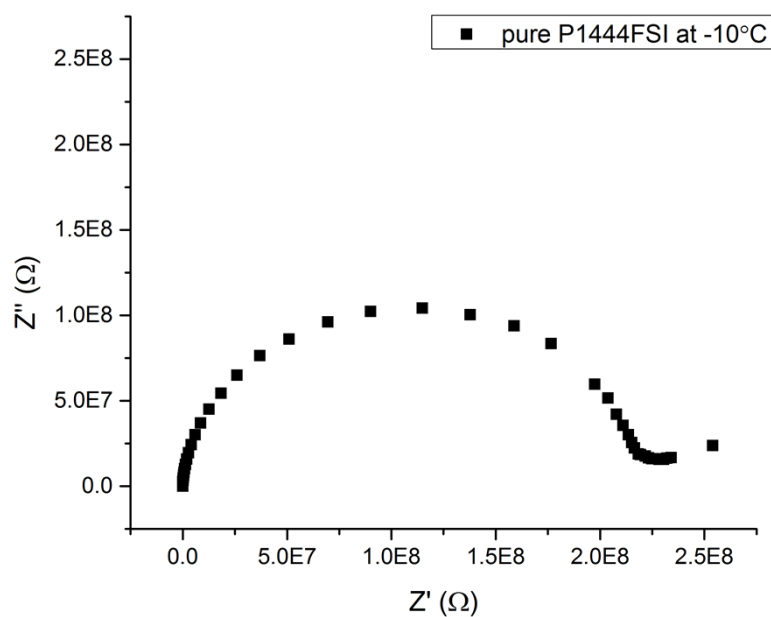


Fig S5 The Nyquist plot of impedance spectrum for pure P₁₄₄₄FSI at -10 °C. The modelled touchdown point was used in Fig 3. The proposed equivalent circuit for this blocking-electrode system consists of a constant phase element in parallel with a resistor, which is attributed to bulk electrolyte resistance. The same model was applied to all spectra.

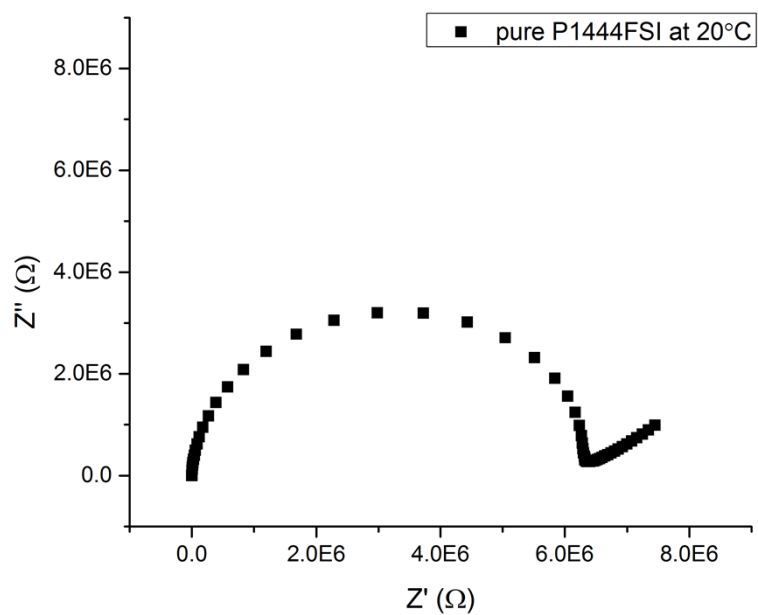


Fig S6 The Nyquist plot of impedance spectrum for pure P₁₄₄₄FSI at 20 °C. The modelled touchdown point was used in Fig 3.

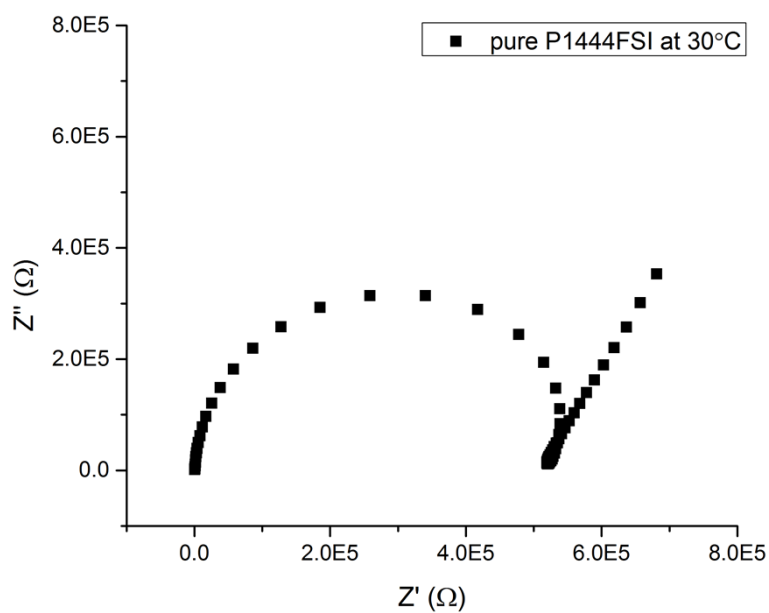


Fig S7 The Nyquist plot of impedance spectrum for pure P₁₄₄₄FSI at 30 °C. The modelled touchdown point was used in Fig 3. Note that this temperature is at the onset of the rapid change of conductivity associated with the Phase I – liquid transition and that this complex phase behaviour may be the origin of the additional feature that appears near the touchdown point.

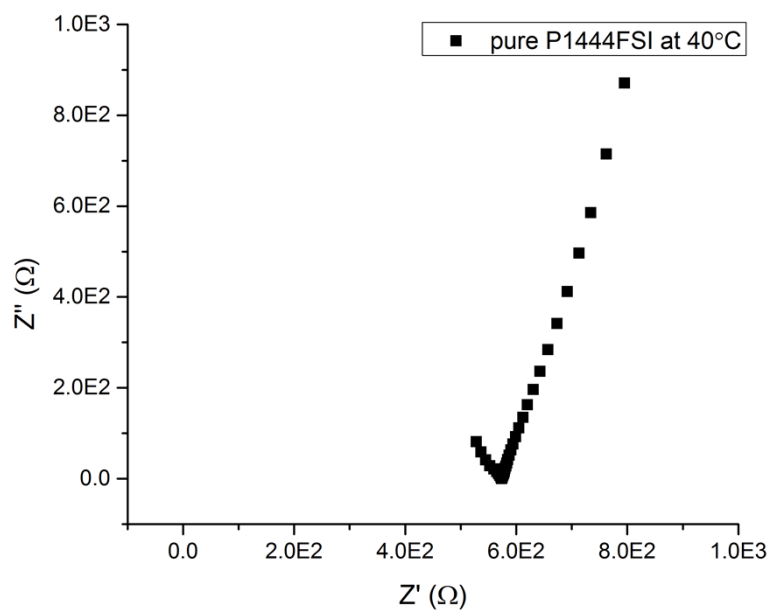


Fig S8 The Nyquist plot of impedance spectrum for pure P₁₄₄₄FSI at 40 °C. The modelled touchdown point was used in Fig 3.

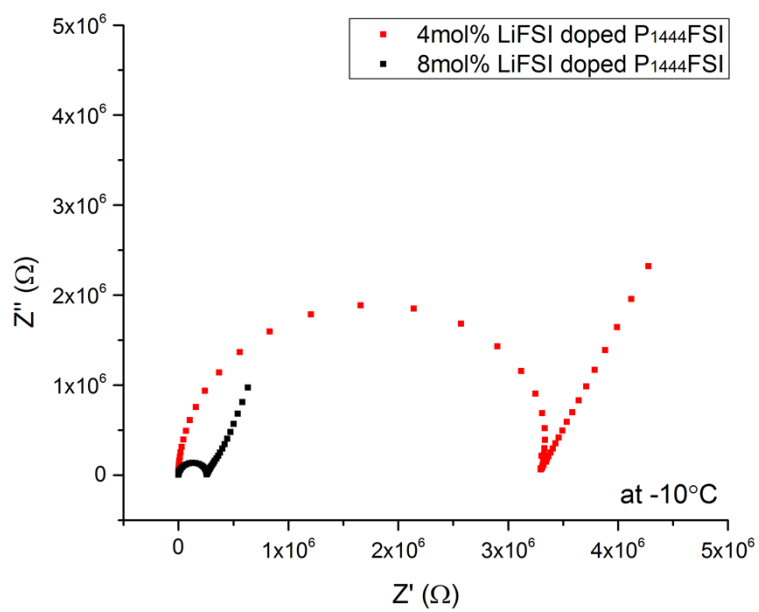


Fig S9 The Nyquist plot of impedance spectra for LiFSI doped P₁₄₄₄FSI at -10 °C. The modelled touchdown point was used in Fig 3.

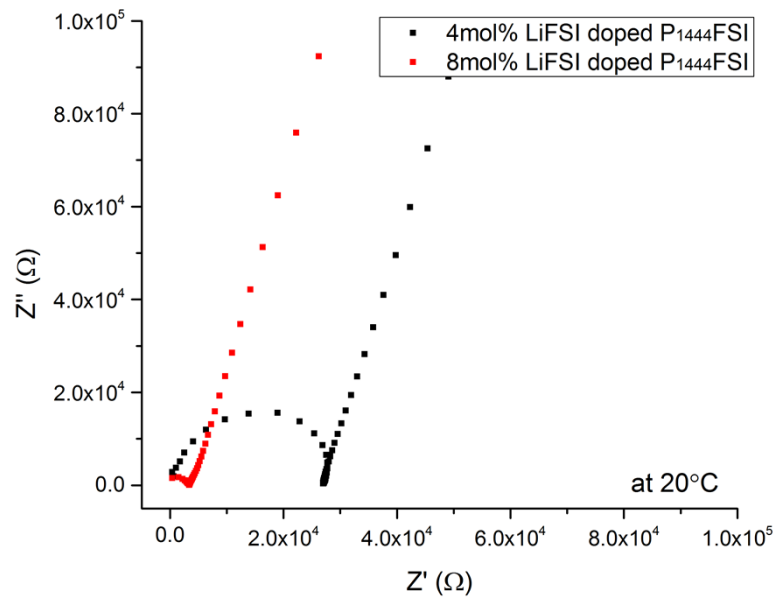


Fig S10 The Nyquist plot of impedance spectra for LiFSI doped P₁₄₄₄FSI at 20 °C. The modelled touchdown point was used in Fig 3.

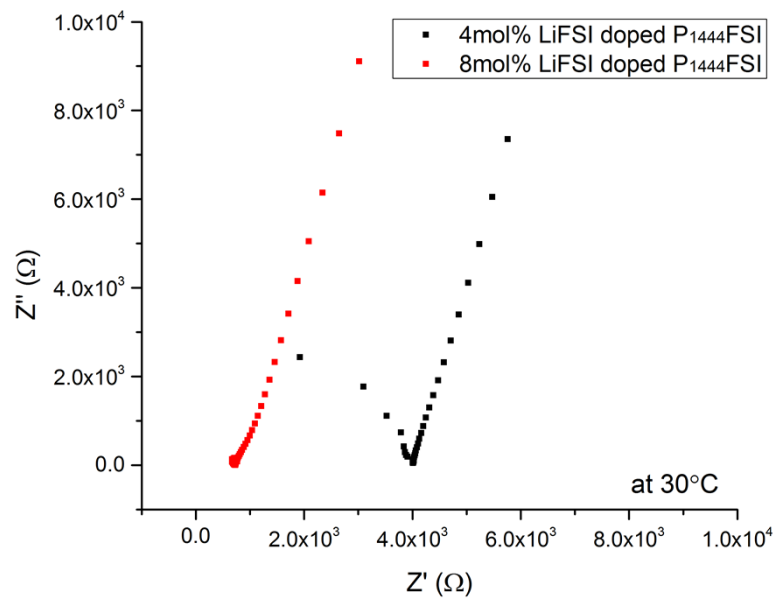


Fig S11 The Nyquist plot of impedance spectra for LiFSI doped P₁₄₄₄FSI at 30 °C. The modelled touchdown point was used in Fig 3.

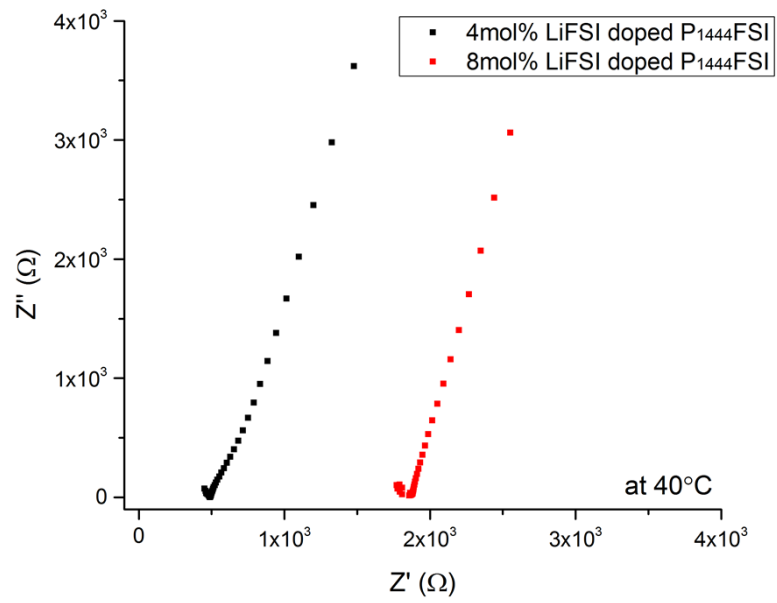


Fig S12 The Nyquist plot of impedance spectra for LiFSI doped P₁₄₄₄FSI at 40 °C. The modelled touchdown point was used in Fig 3.